Manuscript accepted for publication in Computer Methods and Programs in Biomedicine

Analysis and multiclass classification of pathological knee joints using vibroarthrographic signals

Krzysztof Kręcisz,[a,*] Dawid Bączkowicz[a]

[a]Faculty of Physical Education and Physiotherapy, Opole University of Technology, Poland

[*]Corresponding author:

Krzysztof Kręcisz

Faculty of Physical Education and Physiotherapy

Opole University of Technology

ul. Prószkowska 76, 45-758

Opole, Poland.

Electronic mail: k.krecisz@po.opole.pl

ABSTRACT

Background and Objective: Vibroarthrography (VAG) is a method developed for sensitive and objective assessment of articular function. Although the VAG method is still in development, it shows high accuracy, sensitivity and specificity when comparing results obtained from controls and the non-specific, knee-related disorder group. However, the multiclass classification remains practically unknown. Therefore the aim of this study was to extend the VAG method classification to 5 classes, according to different disorders of the patellofemoral joint.

Methods: We assessed 121 knees of patients (95 knees with grade I-III chondromalacia patellae, 26 with osteoarthritis) and 66 knees from 33 healthy controls. The vibroarthrographic signals were collected during knee flexion/extension motion using an acceleration sensor. The genetic search algorithm was chosen to select the most relevant features of the VAG signal for classification. Four different algorithms were used for classification of selected features: logistic regression with automatic attribute selection (*SimpleLogistic* in Weka), multilayer perceptron with sigmoid activation function (*MultilayerPerceptron*), John Platt's sequential minimal optimization algorithm implementation of support vector classifier (*SMO*) and random forest tree (*RandomForest*). The generalization error of classification algorithms was evaluated by stratified 10-fold cross-validation.

Results: We obtained levels of accuracy and AUC metrics over 90%, more than 93% sensitivity and more than 84% specificity for the logistic regression-based method (SimpleLogistic) for a 2-class classification. For the 5-class method, we obtained 69% and 90% accuracy and AUC respectively, and sensitivity and specificity over 91% and 69%.

Conclusions: The results of this study confirm the high usefulness of quantitative analysis of VAG signals based on classification techniques into normal and pathological knees and as a promising tool in classifying signals of various knee joint disorders and their stages.

Keywords: Vibroarthrography; Joint motion quality; Machine learning

1. Introduction

Vibroarthrography (VAG) is an experimental method developed for noninvasive assessment of articular function, especially arthrokinematics. The VAG method is based on the analysis of high frequency vibroacoustic emission, which is a natural phenomenon acquired from the relative motion of articular surfaces of the synovial joint (diarthrosis) [1-3]. In physiological conditions, articular surfaces covered by hyaline cartilage are smooth and slippery, which determines optimal arthrokinematic motion quality [1,4]. In contrast, degenerated cartilage results in greater friction during movement, which is reflected in an increase in amplitude and frequency of the VAG signal [2]. Chondral lesions (such as chondromalacia or osteoarthritis) are often observed in a patellofemoral joint (PFJ), a part of the knee joint complex, which can be explained by its specific biomechanical environment and substantial involvement in daily/sports activity. Due to this but also due to having the greatest susceptibility to the VAG test resulting from a superficial position, the knee is the joint most commonly analyzed by VAG.

Although the VAG method is still in development, it shows high accuracy, sensitivity and specificity, when comparing results obtained from controls and a non-specific, knee-related disorder group [5]. Nalband et al. [6] applied the least square support vector machines algorithm based on the time-complexity parameters of the VAG signal and obtained greater than 94% classification accuracy, greater than 98% sensitivity and 86% specificity [6]. Kim et al. [4] presented classification of the neural network with frequency parameters as inputs, which allowed for improvement of the accuracy to more than 95%, sensitivity 92% and specificity of more than 98% [4]. The best results of the normal-abnormal classification signal are found in the work of Rangayyan et al. [7]. The authors used a classifier based on a radial basis function

network with statistical parameters in the time domain. Here, the accuracy, sensitivity and specificity reached 100%, with the cross-validation of the leave-one-out method [7].

Nevertheless, it should be noted that the mentioned authors based their analysis only on two classes, normal and abnormal. However, from a clinical point of view, the 2-class classification is insufficient for an appropriate diagnostic process and further adequate treatment, and a more specific categorization of chondral-related changes is necessary [8]. Similarly, the radiological staging of chondral disorders (especially early stages, such as chondromalacia) using X-ray also possess significant limitations, due to the low sensitivity and specificity [9]. On the other hand, availability of modern imaging methods such as magnetic resonance imaging (MRI) is limited due to the high expense [9]. Moreover, current diagnostic methods are entirely observer-dependent and require significant knowledge, expertise, and time. Therefore, due to the constantly increasing incidence of age-related cartilage lesions, there have been calls for the development of noninvasive, observer-independent and financially accessible methods for evaluation of human joints, with sensitivity and specificity comparable with MRI, considered the gold standard for chondral lesion assessment.

Recently it has been demonstrated that the VAG method could be helpful in differentiating particular disorders of the PFJ and its stages, due to the specific, disorder-related character of the VAG signal pattern [2,9]. However, while the problem of classification of normal and abnormal VAG signals has been studied, extending it to a multiclass classification remains practically unaddressed. Moreover, as previously suggested, further work is needed to determine whether the sensitivity and specificity of the VAG method are sufficient for clinical application [10].

Furthermore, there is a pressing need for description of optimal algorithms for VAG signal multiclass classification, in accordance with the clinical criteria of PFJ chondral lesions [Nalband]. Optimization of diagnostic methods should include the selection of the most relevant and discriminating VAG signal parameters, followed by selection of an optimal predictive model [11-14]. This will allow us to develop an observer-independent, sensitive, computer-aided diagnostic method, useful for clinicians, in particular for orthopedists and physiotherapists, who are concerned with evaluation of the quality of arthrokinematic motion during physical examination [1].

Thus, the primary goal of our study will be to extend the VAG signal categorization of various PFJ chondral lesions to a 5-class classification (normal and four classes of disorders). Our analyses will be performed with respect to the MRI examination, as a reference method of noninvasive assessment of chondral lesions, which will allow us to evaluate the sensitivity and specificity of the VAG method. For the optimization problem, we applied two algorithms for selecting the best parameters: genetic search and selection based on simple regression functions. Then we compared four classification models representing different approaches to the classification problem: logistic regression with automatic attribute selection based on simple regression functions, multilayer perceptron with sigmoid activation function, sequential minimal optimization algorithm implementation of support vector machine classifier and random forest tree.

The paper is structured as follows: Section 2 describes the analyzed material and the methodology of the study, including the feature extraction techniques, feature selection algorithms and classification methods. Section 3 presents the obtained results, which are discussed in Section 4. Finally, Section 5 presents our conclusions.

2. Materials and methods

2.1. Participants

121 knees from 56 patients with chondromalacia patellae (CMP) (38 with bilateral and 20 with unilateral symptoms) and 16 patients with osteoarthritis (OA) (10 with bilateral and 6 with unilateral symptoms) were enrolled in the study. Knees with CMP were classified into 3 grades according to criteria of the International Cartilage Repair Society by MRI imaging: CMP stage I (28 knees; CMPI), CMP stage II (31 knees; CMPII) and CMP stage III (36 knees; CMPIII) [2,9]. OA patients were selected from clinical/radiological data and the fulfillment of the American College of Rheumatology Subcommittee derived criteria [9]. All patients were recruited from the outpatient populations of the Opole Voivodship Medical Centre, Poland. Both knees from patients with bilateral symptoms were assessed, and only the symptomatic knee from patients with unilateral symptoms was analyzed.

66 knees from 33 healthy volunteers possessing neither knee disorders nor pain (analyzed in the physical examination but without radiological exclusion of the cartilage pathologies) served as a control group (CON). Acute inflammation of the knee joint as well as a history of meniscal tear, knee ligament/tendon ruptures, muscle injuries and traumas excluded individuals from the study. For detailed characteristics of subjects see Table 1.

Qualification for the research and the VAG assessments were performed by the same research team, which included a medical doctor, a senior physiotherapist, a bachelor of physiotherapy and a technician. The project was approved by the Ethics Committee of Opole Voivodship. Signed informed consent was obtained from all tested persons.

TABLE 1. Characteristics of analyzed subjects and knee cases.

	N	*Males/Females*	*Age [years] mean (SD)*	*Height [cm] mean (SD)*	*Weight [kg] mean (SD)*
Subjects					
Controls	33	12/21	37.6 (6.6)	169.2 (7.9)	69.8 (12.2)
With CMP	56	19/37	39.5 (7.2)	168.6 (7.1)	71.9 (12.4)
With OA	16	5/11	41.5 (8.2)	168.6 (8.8)	70.2 (13.8)
Knees					
Controls	66	24/42	-	-	-
With stage I of CMP	28	13/15	-	-	-
With stage II of CMP	31	8/23	-	-	-
With stage III of CMP	36	9/27	-	-	-
With OA	26	8/16	-	-	-

Abbreviations: N, number of cases; CMP, chondromalacia patellae; OA, osteoarthritis

2.2. Experimental Procedure

For each knee, assessment of PFJ quality of motion was performed in an open kinetic chain in flexion/extension motion using an acceleration sensor as described previously [2,9]. Briefly, for each knee, assessment of the VAG signal was performed with a sensor placed, in a seated position, 1 cm above the apex of the patella. The following procedure was performed: (i) loose hanging legs with knees flexed at 90°; (ii) full knee extension from 90° to 0°; (iii) re-flexion (from 0° to 90°) in a sitting position, four times in a 6-second period. Both flexion/extension motion and measuring condition constant velocities were maintained at 82 beats per minute with a metronome. Data were recorded at sampling frequency 10 kHz and then filtered using a fourth-order zero-phase Butterworth band-pass digital filter with cutoff frequencies between 50 Hz and 1000 Hz (Figure 1).

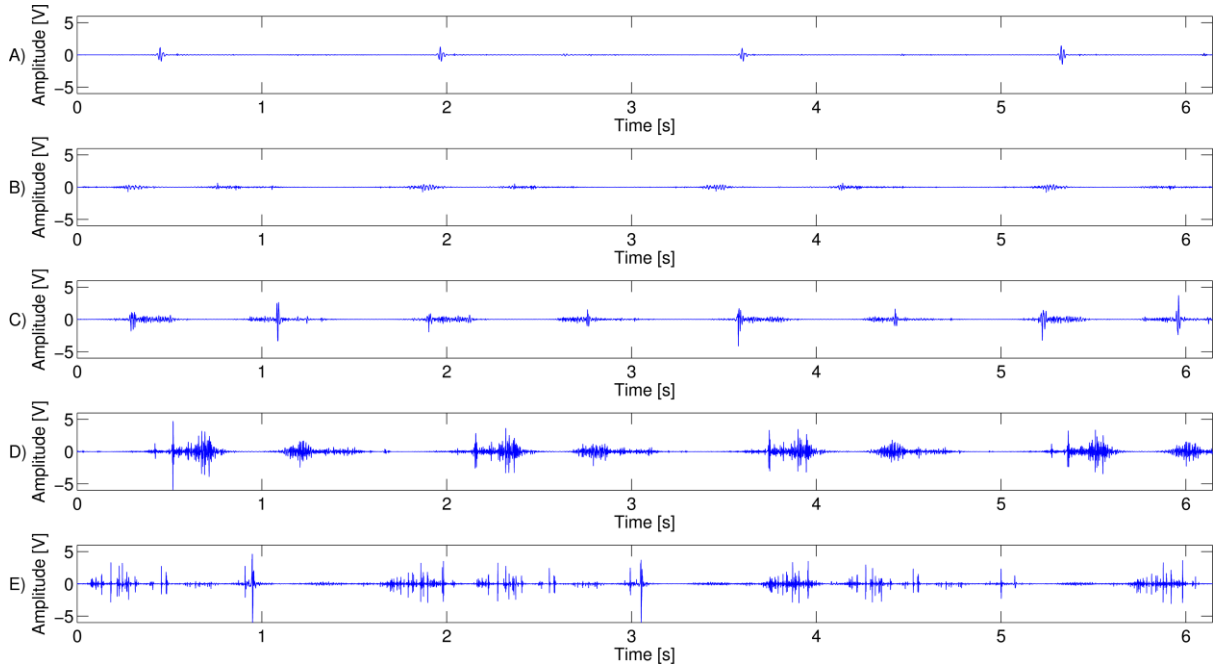

Fig. 1 - Band-pass filtered time series specific for particular group: A) Control, B) CMPI, C) CMPII, D) CMPIII, E) OA.

2.3. Signal feature extraction

The variability of the VAG signal in the time domain was assessed by computing following parameters:

1) the mean-squared values of an obtained signal in fixed-duration segments of 5 ms each and then computing the variance of the values of the parameter over the entire duration of the signal (VMS) [15],

2) signal amplitude was calculated as the difference between the mean of four maximum values and the mean of four minimum VAG signal values (R4) [9].

VMS and R4 were computed using custom made MATLAB (MathWorks, Natick, MA) functions.

The signal complexity was evaluated by several features:

1) form factor (FF) computed as the ratio of mobility of the first derivative of the signal to the mobility of the signal itself (where the mobility denotes the square root of the

ratio of the variance of the first derivative of the signal to the variance of the original signal) [16],

2) Shannon entropy (SHE) based on the probability density function (PDF) of the given signal, denoted by $p_x(x_l)$, with x_l, l = 0, 1, 2, . . . , L − 1, representing L = 248 bins used to represent the range of the values of the signal x and which is a measure of the nature and spread of the PDF and defined as a sum of $p_x(x_l)$ multiplied by log $p_x(x_l)$ [16],

3) turns count (TC) based on detection of changes in amplitude larger than 0.5 times standard deviation of VAG signal [15],

4) the fractal scaling index (DFA) computed with the detrended fluctuation analysis algorithm (time scales from 4 to N/4, where N is the number of VAG signal data points) [17],

5) multiscale sample entropy (MSE) computed over 23 time scales (S7-S30) and area under the sample entropy (m=2 and r=015% of standard deviation) vs. time scale curve (Figure 5) [18].

FF, SHE and TC were computed using the MATLAB WAFO Toolbox (http://www.maths.lth.se/matstat/wafo) and the BIOSIG toolbox (http://biosig.sf.net). DFA and MSE were computed using software available at http://www.physionet.org.

Moreover, we quantified nonlinear information in the VAG signal by recurrence quantification analysis (RQA) [19,20]:

1) recurrence rate (RR), which is measure of the density of recurrence points in a recurrence plot of the phase space trajectory of the system,

2) determinism (DET) quantifies the fraction of recurrent points forming diagonal line structures and refers to the percentage of consecutive recurring points,

3) laminarity (LAM) scores for a fraction of recurrent points forming vertical line structures,

4) entropy (ENT) is defined as the Shannon information entropy of a histogram of diagonal line lengths,

5) trapping time (TT) is the average length of the vertical lines,

6) maxline (LMAX) is the length of the longest diagonal line excluding the main diagonal.

RQA parameters were computed using the PyRQA Python package (https://pypi.python.org/pypi/PyRQA). Parameters of values for RQA were chosen as follows: m=6, time delay=1, radius=10, Theiler corrector=1, distance nom= Euclidean.

The frequency characteristics of the VAG signal were examined by a short-time Fourier transform analysis. The short-time spectra were obtained by computing the discrete Fourier transform of segments, 150 samples each, Hanning window, and 100 samples overlap of each segment. The spectral activity was analyzed by summing spectral power of the VAG signal in two bands: 50–250 Hz (P1) and 250–450 Hz (P2) [9]. Two additional frequency parameters were derived by computing power spectral density at 470 Hz (F470) and 780 Hz (F780) from Fast Fourier Transform of the VAG signal. F470 and F780 were computed using the MATLAB spectrogram function. The extracted features dataset is available at http://doi.org/10.17632/kbt7v3szbj.1.

2.4. Feature selection and classification algorithms

Two types of group classification were performed: 1) 2-class classification Normal/Abnormal, where an abnormal group was formed by grouping CMPI, CMPII,

CMPIII and OA signals, 2) 5-class classification: Controls, CMPI, CMPII, CMPIII and OA. Feature selection and classification tasks were implemented in Weka open-source software [21].

The genetic search algorithm was chosen to select the most relevant features for classification into 3 classifiers: MultilayerPerceptron, SMO and RandomForest (except SimpleLogistic, which has its own automatic attribute selection based on simple regression functions). Weka's *GeneticSearch* implements the simple genetic algorithm described by Goldberg (1989) [22]. This algorithm propagates the best population member to the next generation. The subset evaluator is based on considering the individual predictive ability of each feature along with the degree of redundancy between them [23].

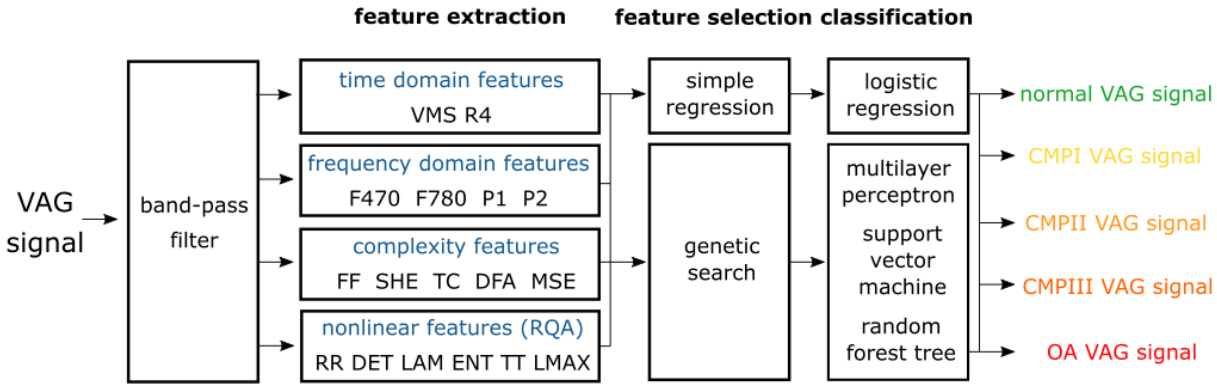

Fig. 2. Block diagram of the classification of the VAG signals. The abbreviations used are defined in Section 2.

For the classification of VAG signals, we used classifiers representing distinct types of algorithms. Four different algorithms were used for classification of selected features: logistic regression with automatic attribute selection (*SimpleLogistic* in Weka), multilayer perceptron with sigmoid activation function (*MultilayerPerceptron* in Weka), John Platt's sequential minimal optimization algorithm implementation of

support vector machine classifier (*SMO* in Weka) and random forest tree (*RandomForest* in Weka). We used default classifier parameters for algorithms in Weka without fine tuning the hyperparameters of the model to minimize the chance of overfitting [24]. The training process of classification algorithms in both 2-class and 5-class classifications was conducted using the 10-fold cross-validation method described in 2.5.

The block diagram of the classification of the VAG signals is shown in Figure 2.

2.5. Classification performance evaluation

The generalization error of classification algorithms was evaluated by stratified 10-fold cross-validation. In this method, one randomly splits the training dataset into 10 folds without replacement, where 9 folds are used for the model training and 1 fold is used for testing. This procedure is repeated 10 times so that we obtain 10 models and performance estimates. The class proportions are preserved in each fold to ensure that each fold is representative of the class proportions in the training dataset. The test results are averaged to estimate the classifier's performance [25].

The performance of classifiers was measured by accuracy, specificity, sensitivity and area under the ROC curve (AUC). According to the confusion matrix for 2 classes, task overall accuracy is defined as ACC=(TP+TN)/(TP+FP+FN+TN), specificity SPEC=TN/(FP+TN) and sensitivity SENS=TP/(TP+FN), where: TP = true positive value, TN = true negative value, FP = false positive value, and FN = false negative value. AUC is defined as the area under the ROC curve which is created by plotting the sensitivity against 1−specificity at various threshold settings. For 5 classes the weighted average metrics were computed, where each target class is weighted according to its prevalence.

3. Results

In this section we describe the results of VAG signal parameterization and selection of the most relevant discriminate parameters and models using software and algorithms which are described in detail in the previous section.

2-class classification

Figure 3 show box plots of all extracted features from normal and abnormal VAG signals. Hotelling's t-squared statistic revealed statistically significant differences between these two groups for VAG measures ($p<0.00001$). Subsequent t-tests showed statistically significant differences ($p<0.00001$) of all parameters except the SHE ($p=0.62120$).

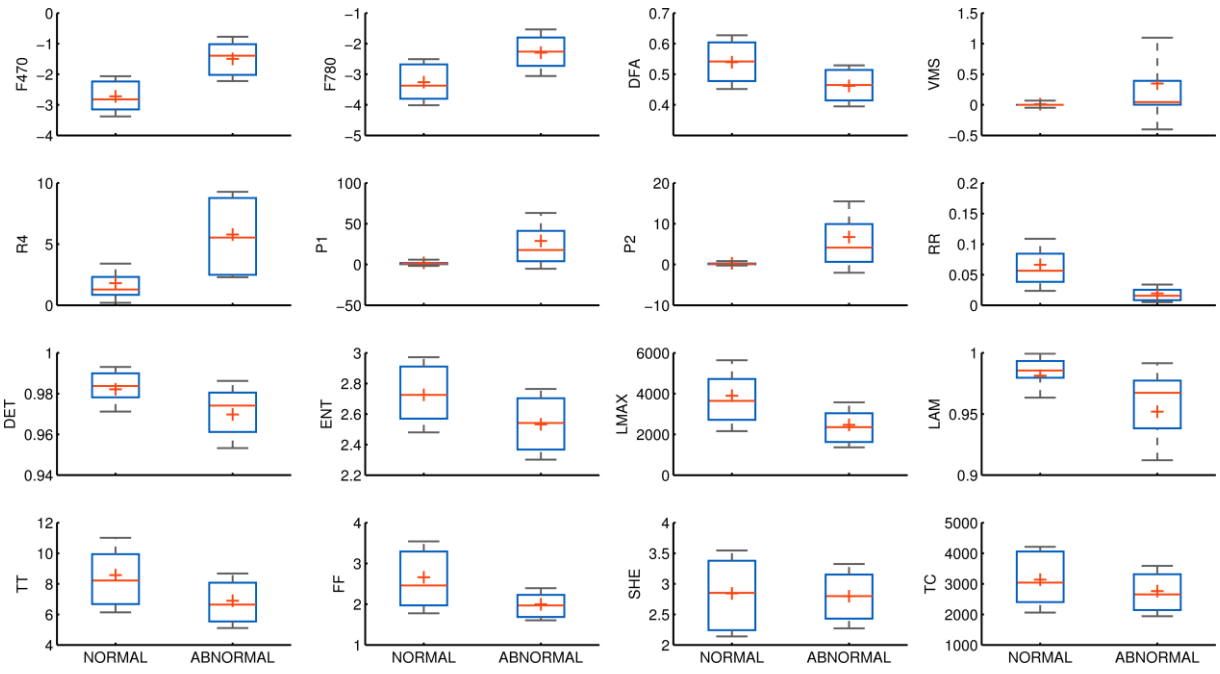

Fig. 3 - Box plots of 16 extracted features of normal – abnormal signals. The horizontal line within the box indicates median, plus marks indicate mean, box boundaries indicate 25th and 75th percentiles, whiskers indicate standard deviations.

A more detailed analysis shows that abnormal signals show higher values of time domain (VMS and R4) and frequency domain (F470, F780, P1 and P2) parameters, lower values of FF, TC, DFA and MSE parameters (complexity features) and lower values of the RQA parameters (RR, DET, LAM, ENT, TT, LMAX). Due to the relatively large amount of data, the exact quantitative values of the VAG signal parameters are shown in Appendix B.

Results of feature selection by the SimpleLogistic regression algorithm and genetic search are presented in Table 2. The SimpleLogistic regression algorithm chooses five features, which might be most relevant to build an effective 2-class classification model (F470, RR, S29, FF, SHE). In turn, using genetic search the F470, F780, P1, P2, RR, DET, LMAX, S14, S30 and FF parameters were selected as the most significant features.

TABLE 2. Feature selection and classification results for 2 classes task (in percents).

Feature selection algorithm	**Selected features**	**Classification model**	**ACC**	**SEN**	**SPE**	**AUC**
SimpleLogistic regression	F470, RR, S29, FF, SHE	SimpleLogistic	90.4	93.4	84.8	95.6
Genetic search	F470, F780, P1, P2, RR, DET, LMAX, S14, S30, FF	MultilayerPerceptron	88.8	91.7	83.3	94.6
		RandomForest	87.2	90.1	81.8	93.6
		SMO	84.5	89.3	75.8	91.9

ACC, accuracy; SEN, sensitivity; SPE, specificity; AUC, area under the ROC curve

The extracted parameters are given as inputs to classifiers, the results of which for each analyzed model are presented in Table 2. All the values of the quality metrics of classification exceed 80%, for the best classification algorithm of SimpleLogistic at the level of 90% and 95% for accuracy and AUC, respectively, and 93% and 85% for sensitivity and specificity, respectively.

3.1. 5-class classification

Distribution of results for 5 classes is similar to the 2 classes with additional trends arising from the existence of multiple classes (Figure 4). Here we have a similar relationship to the case of 2 classes: with 4 classes abnormal signals have higher values of time domain and frequency domain parameters, lower values of all complexity parameters and lower all nonlinear parameters of RQA.

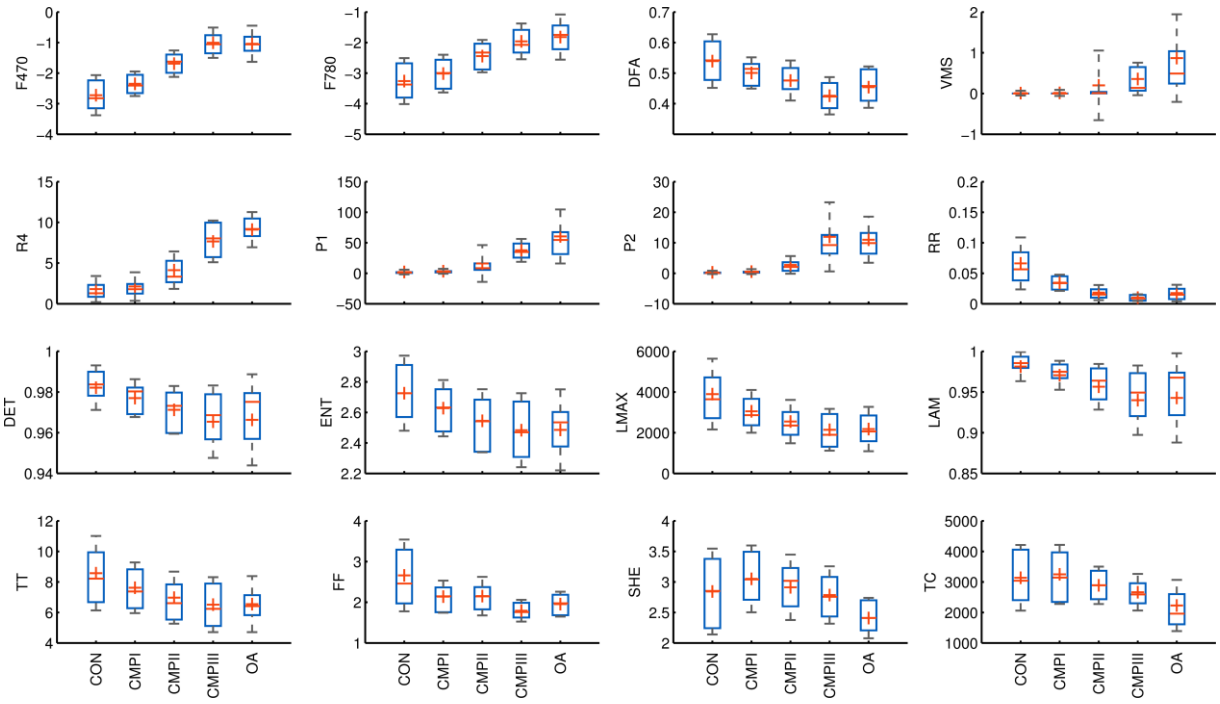

Fig. 4 - Box plots of 16 extracted features of VAG signals for 5 classes (for MSE see Figure 5). The horizontal line within the box indicates median, plus marks indicate mean, box boundaries indicate 25th and 75th percentiles, whiskers indicate standard deviations.

Moreover, there can be observed an increase of power at high frequencies (F470, F780, P1, P2), mean amplitude of the signal (VMS) and the number of high amplitude values (R4) with the severity of joint disorder (from CMPI to OA). In contrast, the complexity of pathological VAG signals is lower than normal signals; DFA, FF and TC values decrease in the order CON, CMPI, CMPII, CMPIII, OA.

Statistical analysis of multivariate analysis of variance (MANOVA) shows main effects statistically significant in all analyzed parameters ($p<0.00001$). The detailed analysis of variance (ANOVA) shows, however, lack of significance in many parameters, particularly in comparisons of CON-CMPI and CMPIII-OA. Detailed results of the analysis of variance are presented in Appendix 2. All statistics were performed using Statistica v.13.1 (StatSoft, Inc., OK, USA).

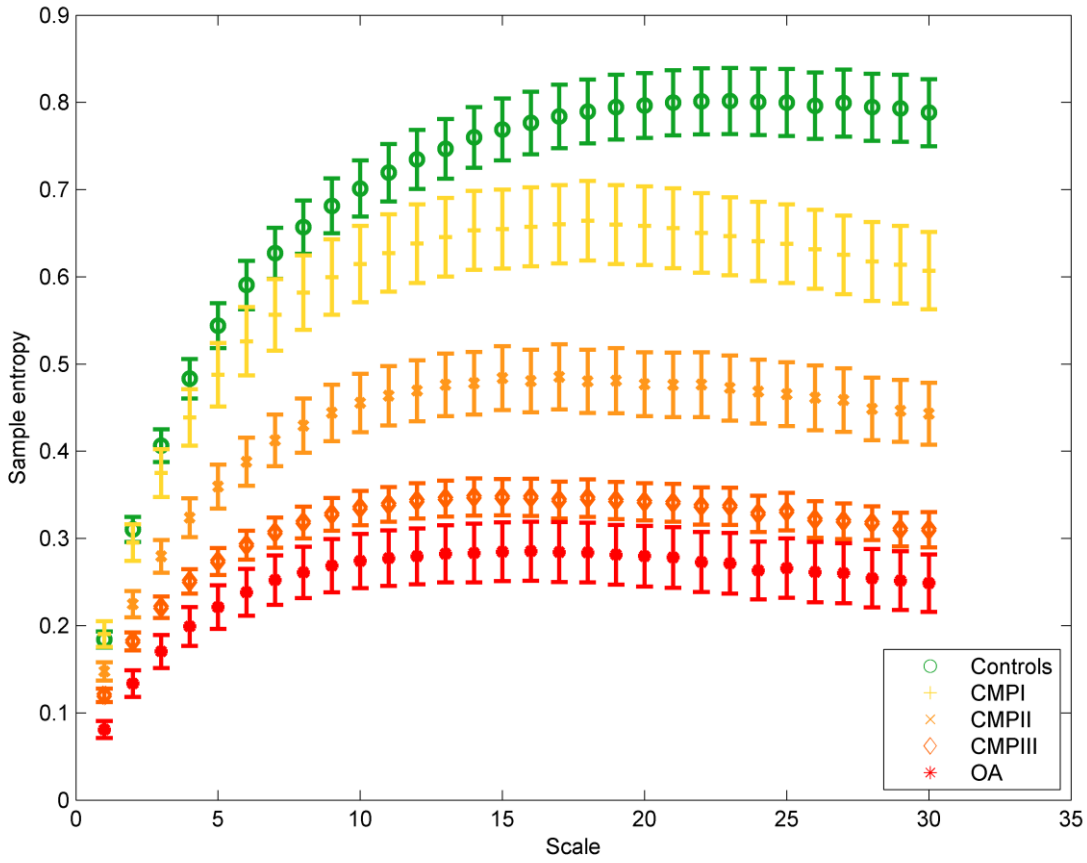

Fig. 5 - Multiscale entropy curves (mean ± standard error) of VAG signals.

Results of feature selection by the SimpleLogistic regression algorithm showed that to build the 5-class classification model the most relevant are frequency domain (F470, F780, P1, P2), time domain (VMS and R4), nonlinearity (RR, DET, TT, LAM) and complexity (FF, DFA, TC, S7, S8, S29, S30) parameters. In turn, genetic search chooses the following parameters, which showed the highest relevance: F470, F780, P1, P2, VMS R4, RR, S14, FF (Table 3).

TABLE 3. Feature selection and classification results for 5 classes task (in percents)

Feature selection algorithm	**Selected features**	**Classification model**	**ACC**	**SEN**	**SPE**	**AUC**
SimpleLogistic regression	F470, F780, VMS, P1, P2, R4, RR, DET, TT, FF, LAM, DFA, TC, S7, S8, S29, S30	SimpleLogistic	69.0	91.4	69.0	90.0
		MultilayerPerceptron	69.0	91.2	69.0	90.2
Genetic search	F470, F780, P1, P2, VMS, R4, RR, S14, FF	RandomForest	62.0	89.7	62.0	89.7
		SMO	61.5	89.0	61.5	89.6

ACC, accuracy; SEN, sensitivity; SPE, specificity; AUC, area under the ROC curve

Similarly to the 2-class classification, for the 5-class classification, the accuracy, AUC, sensitivity and specificity are computed to compare the performance of the classifier (Table 3). The best results were obtained for the SimpleLogistic and MultilayerPerceptron algorithms. These models reached an accuracy rate of 69% and AUC of 90%, with the sensitivity and specificity at the level of 91% and 69% respectively, in both models.

4. Discussion

Results presented in this paper confirm the high usefulness of the quantitative analysis of VAG signals based on classification techniques for normal and pathological knees [4-6,26]. We obtained over 90% levels of accuracy and AUC metrics, more than 93% sensitivity and more than 84% specificity for the logistic regression-based method (SimpleLogistic). These values are slightly lower than those we can find in the published research works, where the values obtained for accuracy, sensitivity and specificity are in the range of 94-100% [4,6,7,11,12]. The slightly worse results we obtained in this work can be partly explained by the inclusion in the abnormal group of participants with PFJ disorders only, whereas in other studies a much wider range of pathologies was analyzed, often only very broadly defined [10,16,23,27,28]. Our findings could also have been influenced by the fact that knees with CMPI are characterized by slight lesions in the articular cartilage, noticeable only in MRI imaging [29,30]. VAG waveforms from these patients are only slightly different from the VAG signals of healthy individuals, and some of them could be interpreted as 'normal'.

However, it should be mentioned that the 2-class classification, despite high rates of accuracy, sensitivity and specificity, is characterized by limited clinical application and can only support screening tests [26]. Therefore, in this study we extended the classification limited to normal and abnormal VAG signals by classifying signals of 4 various knee joint disorders and its stages. For the 5-class classification (control knees added), again using the SimpleLogistic and MultilayerPerceptron models, we obtained values of accuracy and AUC of 69% and 90% respectively, and sensitivity and specificity over 91% and 69%. These values are significantly lower than the corresponding values obtained for the normal-abnormal classification, but

surprisingly well reflect the level of dysfunctions in the knee and correspond with their progress and biomechanical and morphological background. It seems that once again it can be explained by the minor differences in the level of degradation of the cartilage between the two groups. One can see the similarity of the characteristics of the signals CON vs CMPI and CMPIII vs OA, which entails difficulty in a classification of these cases using machine learning. However, it should be noted that in medical diagnosis using typical methods of research (imaging studies and physical examination), the distinction between pathologies also encountered some difficulties, and it is often not clear [29-31]. This is due to the fact, that in CMPI only slight swelling, softening and roughness of cartilage are observed [2]. Therefore, it seems, that in CMPI some impairment of cartilage integrity occurred, however, without a substantial effect on the articular function analyzed by VAG method. In turn, CMPIII is associated with the loss of more than 50% of patellar cartilage thickness, which brings it closer to the OA, where also is observed the loss of the articular cartilage, but with bone exposure and the narrowing of the joint space [2]. Taken together, the results of our study show that there is an increase of power at high frequencies (F470, F780, P1, P2), mean amplitude of the signal (VMS) and the number of high amplitude values (R4) with the severity of joint disorder (from CMPI to OA). As previously suggested, this phenomenon may be associated with progress of degenerative changes within chondral structures and declining lubrication of articular surfaces, leading to limited possibilities of reducing friction [2].

On the other hand, the complexity of pathological VAG signals is lower than signals of normal joints. DFA, FF and TC values decrease in the order CON, CMPI, CMPII, CMPIII, OA, which corresponds to a progressive disorder, ranging from healthy joints to the most severe changes in the form of knee OA. It is also noted that

the degree of chondral pathology corresponds to the regularity of the signal (MSE), which may, however, result from the characteristics of the algorithm for calculating multiscale sample entropy. Namely, the MSE algorithm is sensitive to outliers of the signal [18]. In pathological signals, we can observe a larger number of high-amplitude vibrations, and this may affect MSE. Thus this parameter should be interpreted in the context not of the signal regularity but the incidence of extreme vibrations.

The selected parameters in the selection process of a classification algorithm indicate the complex, nonlinear nature of VAG signals. Nonlinear characteristics of VAG signals indicate a greater contribution of stochastic components to the pathological signal (RR), a smaller contribution of deterministic components (DET), a smaller number of similar states in which vibrations remain in time (intermittency) (LAM) and less time in which these states occur (TT) [6,19].

Of particular interest is the fact that we obtained the best accuracy for the SimpleLogistic algorithm [32]. Logistic regression is a very widely used method of analysis for classification problems. This is due to the fact that this method offers a relatively clear interpretation of the results. The logistic function has useful properties: it describes the probability of developing the degree of the pathology and has a property of threshold function that is particularly useful in medical and epidemiological studies. The SimpleLogistic algorithm used in this study is a modified and improved version of the logistic regression containing the automatic selection of the best parameters for classification. However, when considering only the 5-class classification the MultilayerPerceptron algorithm based on features chosen by genetic search ensures similar performance of the classification. It therefore seems that for multiclass classification of the VAG signals the most relevant of the parameters described above are frequency domain (F470, F780, P1 and P2), time domain (VMS,

R4), nonlinear (RR) and complexity (FF) features. This finding may be relevant to the final application of analysis of VAG signals for clinical use.

Limitations of the current study are the relatively small sample sizes per group and unequal sex distribution. However, it should be emphasized that these proportions are in agreement with the observed incidence rate of knee lesions. Another limitation is the fact that the inclusion criteria for the control group were an interview and functional testing, indicating the absence of any disturbances in the knee joints, which, however, was not confirmed by MRI procedures. Therefore we cannot exclude that the knees of control subjects possess minor asymptomatic cartilage changes which could also affect our results.

5. Conclusion

In conclusion, we found that the VAG method seems to be sensitive enough for evaluating the biomechanical and morphological changes within the knee joint environment. Analysis and the 5-class classification of the VAG signals give satisfactory results not only for the screening tests but also for classifying signals of various knee joint disorders and their stages, according to the level of chondral lesion [33,34]. Thus, the VAG method may constitute a helpful tool for clinicians and may be implemented as a computer-aided decision support system. In the latter case, further studies are needed that focus on the development of methods for signal analysis in classification of a wide range of VAG signals, also from the other joints. It seems important to focus on all aspects of this method: measurement tools, methods of analysis and selection of classification algorithms, but also simplify the whole assessment procedure [5,6,35-36].

Acknowledgments

We would like to thank all of the subjects who participated in the study.

The project was approved by the Ethics Committee of Opole Voivodship. Signed informed consent was obtained from all tested persons.

The authors declare no conflict of interest.

The authors report no external funding source for this study.

REFERENCES

[1] D. Bączkowicz, K. Falkowski, E. Majorczyk, Assessment of Relationships Between Joint Motion Quality and Postural Control in Patients With Chronic Ankle Joint Instability, J. Orthop. Sport. Phys. Ther. 47 (2017) 570–577, doi:10.2519/jospt.2017.6836.

[2] D. Bączkowicz, E. Majorczyk, Joint Motion Quality in Chondromalacia Progression Assessed by Vibroacoustic Signal Analysis, Pm&r. 8 (2016) 1065–1071, doi:10.1016/j.pmrj.2016.03.012.

[3] D. Bączkowicz, E. Majorczyk, K. Kręcisz, Age-Related Impairment of Quality of Joint Motion in Vibroarthrographic Signal Analysis, Biomed Res. Int. 2015 (2015) 1–7, doi:10.1155/2015/591707.

[4] K. Kim, J. Seo, C. Song. Classification of normal and abnormal knee joint using back-propagation neural network, Proc. 2008 Int. Conf. Bioinforma. Comput. Biol. BIOCOMP. 2008 (2008) 483–488.

[5] Y. Wu, Knee Joint Vibroarthrographic Signal Processing and Analysis, SpringerBriefs in Bioengineering. (2015), doi:10.1007/978-3-662-44284-5.

[6] S. Nalband, A. Sundar, A.A. Prince, A. Agarwal, Feature selection and classification methodology for the detection of knee-joint disorders, Comput. Methods Programs Biomed. 127 (2016) 94–104, doi:10.1016/j.cmpb.2016.01.020.

[7] R.M. Rangayyan, F. Oloumi, Y. Wu, S. Cai, Fractal analysis of knee-joint vibroarthrographic signals via power spectral analysis, Biomed. Signal Process. Control. 8 (2013) 23–29, doi:10.1016/j.bspc.2012.05.004.

[8] G. McCoy, J. McCrea, D. Beverland, W. Kernohan, R. Mollan, Vibration arthrography as a diagnostic aid in diseases of the knee. A preliminary report, J Bone Jt. Surg Br. 69-B (2) (1987) 288-293, doi:10.1016/0268-0033(87)90023-4.

[9] D. Bączkowicz, E. Majorczyk, Joint motion quality in vibroacoustic signal analysis for patients with patellofemoral joint disorders, BMC Musculoskelet. Disord. 15 (2014), doi:10.1186/1471-2474-15-426.

[10] Y. Wu, P. Chen, X. Luo, H. Huang, L. Liao, Y. Yao, et al., Quantification of knee vibroarthrographic signal irregularity associated with patellofemoral joint cartilage pathology based on entropy and envelope amplitude measures, Comput. Methods Programs Biomed. 130 (2016) 1–12. doi:10.1016/j.cmpb.2016.03.021.

[11] E. Petre, D. Selişteanu, D. Şendrescu, C. Ionete, Neural networks-based adaptive control for a class of nonlinear bioprocesses, Neural Computing and Applications. 19 (2009) 169–178. doi:10.1007/s00521-009-0284-9.

[12] J. Li and S. M. R. Hasan, Design and Performance Analysis of a 866-MHz Low-Power Optimized CMOS LNA for UHF RFID, IEEE Trans Ind Electron. 60 (2013) 1840-1849. doi: 10.1109/TIE.2012.

[13] R.-E. Precup, R.-C. David, E.M. Petriu, S. Preitl, M.-B. Rădac, Novel Adaptive Charged System Search algorithm for optimal tuning of fuzzy controllers, Expert Syst Appl. 41 (2014) 1168–1175. doi:10.1016/j.eswa.2013.07.110.

[14] S. B. Ghosn, F. Drouby, H. M. Harmanani, A parallel genetic algorithm for the open-shop scheduling problem using deterministic and random moves, Int J Artif Intell. 14 (2016), 130-144. DOI: 10.1145/1639809.1639841.

[15] R.M. Rangayyan, Y. Wu, Analysis of Vibroarthrographic Signals with Features Related to Signal Variability and Radial-Basis Functions, Ann. Biomed. Eng. 37 (2009) 156–163. doi:10.1007/s10439-008-9601-1.

[16] R.M. Rangayyan, Y.F. Wu, Screening of knee-joint vibroarthrographic signals using statistical parameters and radial basis functions, Med. Biol. Eng. Comput. 46 (2008) 223–232. doi:10.1007/s11517-007-0278-7.

[17] C.-K. Peng, S.V. Buldyrev, S. Havlin, M. Simons, H.E. Stanley, A.L. Goldberger, Mosaic organization of DNA nucleotides, Phys. Rev. E 49 (1994) 1685–1689. doi:10.1103/physreve.49.1685.

[18] M. Costa, A.L. Goldberger, C.-K. Peng, Multiscale entropy analysis of biological signals, Phys. Rev. E 71 (2005). doi:10.1103/physreve.71.021906.

[19] N. Marwan, N. Wessel, U. Meyerfeldt, A. Schirdewan, J. Kurths, Recurrence-plot-based measures of complexity and their application to heart-rate-variability data, Phys. Rev. E 66 (2002). doi:10.1103/physreve.66.026702.

[20] C.L. Webber, J.P. Zbilut. Dynamical assessment of physiological systems and states using recurrence plot strategies, J. Appl. Physiol. 76 (1994) 965–973.

[21] M. Hall, E. Frank, G. Holmes, B. Pfahringer, P. Reutemann, I.H. Witten, The WEKA data mining software, ACM SIGKDD Explorations Newsletter. 11 (2009) 10. doi:10.1145/1656274.1656278.

[22] D.E. Goldberg, Genetic algorithms in search, optimization, and machine learning, Addison-Wesley Longman Publishing Co., Inc., 1989.

[23] M. Hall, Correlation-based Feature Selection for Machine Learning, PhD dissertation, Department of Computer Science, University of Waikato, 1999.

[24] P. Domingos, A few useful things to know about machine learning, Commun. ACM 55 (2012) 78. doi:10.1145/2347736.2347755.

[25] R. Kohavi, A Study of Cross-Validation and Bootstrap for Accuracy Estimation and Model Selection, Proceedings of IJCAI. 14 (1995) 1137-1145.

[26] R.M. Rangayyan, Y. Wu, Screening of knee-joint vibroarthrographic signals using probability density functions estimated with Parzen windows, Biomed. Signal Process. Control 5 (2010) 53–58. doi:10.1016/j.bspc.2009.03.008.

[27] D. Moreira, J. Silva, M. Correia, M. Massada, Classification of knee arthropathy with accelerometer-based vibroarthrography. Stud Health Technol Inform. 224 (2016) 33-9. doi: 10.3233/978-1-61499-653-8-33.

[28] C.-S. Shieh, C.-D. Tseng, L.-Y. Chang, W.-C. Lin, L.-F. Wu, H.-Y. Wang, P.-J. Chao, C.-L. Chiu, T.-F. Lee, Synthesis of vibroarthrographic signals in knee osteoarthritis diagnosis training, BMC Res Notes. 9 (2016). doi:10.1186/s13104-016-2156-6.

[29] H.K. Pihlajamäki, P.-I. Kuikka, V.-V. Leppänen, M.J. Kiuru, V.M. Mattila, Reliability of Clinical Findings and Magnetic Resonance Imaging for the Diagnosis of Chondromalacia Patellae, J Bone Jt. Surg Am. 92 (2010) 927–934. doi:10.2106/jbjs.h.01527.

[30] M. Samim, E. Smitaman, D. Lawrence, H. Moukaddam, MRI of anterior knee pain. Skeletal Radiol. 43 (2014) 875–893. doi:10.1007/s00256-014-1816-7.

[31] N. Tanaka, M. Hoshiyama, Vibroarthrography in patients with knee arthropathy, J Back Musculoskelet Rehabil. 25 (2012) 117–122. doi:10.3233/bmr-2012-0319.

[32] N. Landwehr, M. Hall, E. Frank, Logistic Model Trees, Mach Learn. 59 (2005) 161–205. doi:10.1007/s10994-005-0466-3.

[33] T. Mu, A.K. Nandi, R.M. Rangayyan, Screening of knee-joint vibroarthrographic signals using the strict 2-surface proximal classifier and genetic algorithm, Comput. Biol. Med. 38 (2008) 1103–1111. doi:10.1016/j.compbiomed.2008.08.009.

[34] Z.M.K. Maussavi, R.M. Rangayyan, G.D. Bell, C.B. Frank, K.O. Ladly, Screening of vibroarthrographic signals via adaptive segmentation and linear prediction modeling, IEEE Trans. Biomed. Eng. 43 (1996) 15. doi:10.1109/10.477697.

[35] S. Cai, S. Yang, F. Zheng, M. Lu, Y. Wu, S. Krishnan, Knee Joint Vibration Signal Analysis with Matching Pursuit Decomposition and Dynamic Weighted Classifier Fusion, Comput. Math. Methods Med. 2013 (2013) 1–11. doi:10.1155/2013/904267.

[36] Y. Wu, S. Krishnan, Combining least-squares support vector machines for classification of biomedical signals: a case study with knee-joint vibroarthrographic signals, J. Exp. Theor. Artif. Intell. 23 (2011) 63–77. doi:10.1080/0952813x.2010.506288.

Appendix A

Effects of selecting a learning algorithm based on Bayesian optimization methods and random search over its hyperparameters - Auto-WEKA package [1].

Auto-WEKA result for 2-class classification:

------- 5 BEST CONFIGURATIONS -------

Configuration #1:

Scheme: weka.classifiers.meta.Bagging -P 58 -S 1 -num-slots 1 -I 13 -W weka.classifiers.functions.MultilayerPerceptron -- -L 0.8537172390233696 -M 0.6032267313055338 -N 500 -V 0 -S 1 -E 20 -H t -B -C –R

Configuration #2:

Scheme: weka.classifiers.functions.MultilayerPerceptron -L 0.7124792551054612 -M 0.19142401626579603 -N 500 -V 0 -S 1 -E 20 -H i

Configuration #3:

Scheme: weka.classifiers.meta.AttributeSelectedClassifier -E "weka.attributeSelection.CfsSubsetEval -P 1 -E 1" -S "weka.attributeSelection.GreedyStepwise -T -1.7976931348623157E308 -N -1 -num-slots 1" -W weka.classifiers.functions.SGD -- -F 1 -L 0.006829365910517769 -R 2.0894080667955306E-11 -E 500 -C 0.001 -S 1

Configuration #4:

Scheme: weka.classifiers.functions.SimpleLogistic -I 0 -M 500 -H 50 -W 0.0

Configuration #5:

Scheme: weka.classifiers.meta.AttributeSelectedClassifier -E "weka.attributeSelection.CfsSubsetEval -P 1 -E 1" -S "weka.attributeSelection.GreedyStepwise -T -1.7976931348623157E308 -N -1 -num-slots 1" -W weka.classifiers.functions.SMO -- -C 1.1258189038152562 -L 0.001 -P 1.0E-12 -N 0 -V -1 -W 1 -K "weka.classifiers.functions.supportVector.Puk -O 0.30763920387688776 -S 6.850211869028438 -C 250007"

TABLE 1. Auto-WEKA classification results for 2 classes task (in percents).

Classifier	Accuracy	Sensitivity	Specificity	AUC
Configuration #1	87.7	90.9	81.8	96.0
Configuration #2	87.7	90.9	81.8	92.8
Configuration #3	82.9	86.8	75.8	92.9
Configuration #4	89.8	91.7	86.4	96.2
Configuration #5	85.0	92.6	71.2	81.9

Auto-WEKA result for 5-class classification:

------- 5 BEST CONFIGURATIONS -------

Configuration #1:

Scheme: weka.classifiers.functions.MultilayerPerceptron -L 0.39398546524785105 -M 0.3728386586322857 -N 500 -V 0 -S 1 -E 20 -H i

Configuration #2:

Scheme: weka.classifiers.trees.LMT -I -1 -M 15 -W 0.0

Configuration #3:

Scheme: weka.classifiers.meta.AdaBoostM1 -P 86 -S 1 -I 2 -W weka.classifiers.functions.MultilayerPerceptron -- -L 0.9527983201131888 -M 0.11434412042979779 -N 500 -V 0 -S 1 -E 20 -H o

Configuration #4:

Scheme: weka.classifiers.meta.AttributeSelectedClassifier -E "weka.attributeSelection.CfsSubsetEval -P 1 -E 1" -S "weka.attributeSelection.GreedyStepwise -T -1.7976931348623157E308 -N -1 -num-slots 1" -W weka.classifiers.meta.RandomSubSpace -- -P 0.7664967488071254 -S 1 -num-slots 1 -I 2 -W weka.classifiers.trees.LMT -- -I -1 -M 1 -W 0.0

Configuration #5:

Scheme: weka.classifiers.meta.Vote -S 1 -B "weka.classifiers.meta.AttributeSelectedClassifier -E \"weka.attributeSelection.CfsSubsetEval

-P 1 -E 1\" -S \"weka.attributeSelection.BestFirst -D 1 -N 5\" -W weka.classifiers.functions.MultilayerPerceptron -- -L 0.3 -M 0.4517117729945054 -N 500 -V 0 -S 1 -E 20 -H a" -B "weka.classifiers.meta.AttributeSelectedClassifier -E \"weka.attributeSelection.CfsSubsetEval -P 1 -E 1\" -S \"weka.attributeSelection.BestFirst -D 1 -N 5\" -W weka.classifiers.trees.RandomTree -- -K 2 -M 40.0 -V 0.001 -S 1 -depth 9 -N 4" -B "weka.classifiers.meta.AttributeSelectedClassifier -E \"weka.attributeSelection.CfsSubsetEval -P 1 -E 1\" -S \"weka.attributeSelection.BestFirst -D 1 -N 7\" -W weka.classifiers.trees.J48 -- -C 0.7186004 -M 56" -B "weka.classifiers.meta.AttributeSelectedClassifier -E \"weka.attributeSelection.CfsSubsetEval -P 1 -E 1\" -S \"weka.attributeSelection.BestFirst -D 1 -N 7\" -W weka.classifiers.functions.MultilayerPerceptron -- -L 0.9589876515699867 -M 0.4298494794278802 -N 500 -V 1 -S 1 -E 20 -H o" -R AVG"weka.attributeSelection.GreedyStepwise -T -1.7976931348623157E308 -N -1 -num-slots 1" -W weka.classifiers.functions.SMO -- -C 1.1258189038152562 -L 0.001 -P 1.0E-12 -N 0 -V -1 -W 1 -K "weka.classifiers.functions.supportVector.Puk -O 0.30763920387688776 -S 6.850211869028438 -C 250007"

TABLE 2. Auto-WEKA classification results for 5 classes task (in percents).

Classifier	Accuracy	Sensitivity	Specificity	AUC
Configuration #1	67.9	91.9	67.9	91.2
Configuration #2	69.0	91.4	69.0	90.0
Configuration #3	66.8	92.4	66.8	84.7
Configuration #4	60.4	88.0	60.4	87.5
Configuration #5	63.1	86.8	63.1	89.1

[1] C. Thornton, F. Hutter, H.H. Hoos, K. Leyton-Brown, Auto-WEKA: Combined Selection and Hyperparameter Optimization of Classification Algorithms.

Appendix B

Descriptives

Variable	Normal			Abnormal			Controls			CMPI			CMPII			CMPIII			OA		
	Mean	Median	Std. dev.	Mean	Median	Std. dev.	Mean	Median	Std. dev.	Mean	Median	Std. dev.	Mean	Median	Std. dev.	Mean	Median	Std. dev.	Mean	Median	Std. dev.
F470	-2.720	-2.821	0.657	-1.498	-1.395	0.725	-2.720	-2.821	0.657	-2.349	-2.406	0.402	-1.690	-1.625	0.433	-1.005	-1.056	0.496	-1.038	-1.057	0.593
F780	-3.260	-3.373	0.752	-2.297	-2.261	0.761	-3.260	-3.373	0.752	-3.014	-2.997	0.618	-2.442	-2.325	0.531	-1.959	-2.074	0.584	-1.819	-1.746	0.739
DFA	0.539	0.542	0.088	0.462	0.465	0.067	0.539	0.542	0.088	0.501	0.514	0.051	0.476	0.476	0.066	0.426	0.423	0.061	0.454	0.458	0.068
VMS	0.011	0.000	0.059	0.348	0.045	0.749	0.011	0.000	0.059	0.016	0.001	0.075	0.200	0.009	0.854	0.357	0.137	0.398	0.869	0.489	1.076
R4	1.803	1.293	1.601	5.786	5.534	3.493	1.803	1.293	1.601	2.121	1.795	1.754	4.130	3.330	2.303	7.664	8.031	2.561	9.106	9.184	2.167
P1	2.109	1.042	3.873	28.972	17.750	34.275	2.109	1.042	3.873	3.272	2.291	3.962	15.985	8.348	30.107	37.533	34.832	18.790	60.281	54.605	44.340
P2	0.290	0.102	0.537	6.731	4.148	8.754	0.290	0.102	0.537	0.527	0.390	0.816	2.737	2.081	2.898	11.919	9.238	11.327	10.990	9.880	7.546
RR	0.066	0.056	0.043	0.019	0.015	0.014	0.066	0.056	0.043	0.034	0.034	0.013	0.018	0.015	0.012	0.010	0.009	0.006	0.018	0.015	0.013
DET	0.982	0.984	0.011	0.970	0.974	0.016	0.982	0.984	0.011	0.977	0.980	0.009	0.971	0.973	0.012	0.965	0.969	0.018	0.966	0.975	0.022
ENT	2.726	2.725	0.246	2.533	2.541	0.231	2.726	2.725	0.246	2.628	2.632	0.185	2.545	2.541	0.207	2.483	2.470	0.242	2.485	2.534	0.265
LMAX	3897.667	3644.500	1737.771	2466.702	2355.000	1103.619	3897.667	3644.500	1737.771	3052.250	2864.500	1051.594	2550.323	2355.000	1065.823	2145.889	1899.500	1027.223	2180.615	2065.000	1088.813
LAM	0.981	0.986	0.018	0.952	0.967	0.040	0.981	0.986	0.018	0.971	0.975	0.018	0.956	0.964	0.028	0.940	0.949	0.043	0.943	0.968	0.055
TT	8.572	8.218	2.439	6.891	6.638	1.786	8.572	8.218	2.439	7.619	7.375	1.661	6.970	6.608	1.705	6.508	6.239	1.801	6.544	6.412	1.836
MSE	20.830	20.216	7.849	11.743	10.360	6.259	20.830	20.216	7.849	17.512	16.710	6.722	12.856	11.683	5.313	9.326	8.987	3.328	7.550	5.705	4.933
S7	0.627	0.612	0.237	0.380	0.343	0.198	0.627	0.612	0.237	0.556	0.525	0.225	0.412	0.372	0.165	0.307	0.304	0.104	0.252	0.191	0.155
S8	0.657	0.639	0.247	0.395	0.354	0.207	0.657	0.639	0.247	0.582	0.552	0.233	0.429	0.378	0.174	0.318	0.315	0.109	0.261	0.201	0.161
S9	0.681	0.659	0.254	0.408	0.365	0.213	0.681	0.659	0.254	0.600	0.565	0.238	0.444	0.395	0.180	0.328	0.328	0.113	0.269	0.210	0.167
S10	0.701	0.675	0.261	0.417	0.377	0.218	0.701	0.675	0.261	0.615	0.576	0.240	0.455	0.412	0.186	0.335	0.330	0.117	0.274	0.214	0.171
S11	0.719	0.683	0.267	0.424	0.384	0.223	0.719	0.683	0.267	0.627	0.592	0.243	0.464	0.418	0.190	0.339	0.342	0.119	0.277	0.218	0.174
S12	0.735	0.699	0.274	0.430	0.379	0.227	0.735	0.699	0.274	0.638	0.599	0.246	0.469	0.424	0.194	0.343	0.342	0.121	0.280	0.221	0.175
S13	0.747	0.710	0.278	0.435	0.384	0.230	0.747	0.710	0.278	0.645	0.605	0.247	0.476	0.423	0.200	0.346	0.343	0.123	0.282	0.220	0.179
S14	0.760	0.726	0.282	0.438	0.396	0.233	0.760	0.726	0.282	0.653	0.617	0.248	0.478	0.427	0.200	0.348	0.340	0.128	0.283	0.214	0.184
S15	0.769	0.735	0.288	0.440	0.393	0.234	0.769	0.735	0.288	0.655	0.620	0.248	0.484	0.430	0.203	0.347	0.340	0.125	0.285	0.210	0.184
S16	0.776	0.748	0.291	0.440	0.390	0.234	0.776	0.748	0.291	0.657	0.628	0.247	0.481	0.433	0.200	0.347	0.330	0.128	0.285	0.211	0.186
S17	0.784	0.748	0.296	0.441	0.390	0.238	0.784	0.748	0.296	0.660	0.633	0.247	0.485	0.442	0.208	0.344	0.329	0.126	0.284	0.214	0.189
S18	0.790	0.749	0.298	0.441	0.379	0.238	0.790	0.749	0.298	0.664	0.641	0.250	0.480	0.431	0.201	0.346	0.321	0.129	0.284	0.212	0.187
S19	0.795	0.758	0.302	0.439	0.382	0.238	0.795	0.758	0.302	0.660	0.630	0.247	0.481	0.445	0.208	0.344	0.315	0.129	0.281	0.209	0.188
S20	0.796	0.764	0.303	0.436	0.380	0.237	0.796	0.764	0.303	0.659	0.637	0.247	0.477	0.450	0.204	0.342	0.314	0.128	0.280	0.213	0.190
S21	0.800	0.776	0.304	0.435	0.380	0.239	0.800	0.776	0.304	0.656	0.639	0.250	0.476	0.434	0.206	0.341	0.317	0.131	0.278	0.202	0.191
S22	0.801	0.768	0.308	0.432	0.379	0.238	0.801	0.768	0.308	0.650	0.633	0.250	0.476	0.446	0.207	0.337	0.312	0.128	0.273	0.209	0.189
S23	0.802	0.769	0.308	0.429	0.377	0.237	0.802	0.769	0.308	0.647	0.637	0.245	0.473	0.442	0.208	0.337	0.316	0.128	0.271	0.205	0.190
S24	0.801	0.770	0.309	0.423	0.365	0.236	0.801	0.770	0.309	0.641	0.626	0.249	0.468	0.448	0.204	0.328	0.309	0.125	0.263	0.200	0.181
S25	0.800	0.775	0.312	0.422	0.371	0.235	0.800	0.775	0.312	0.638	0.618	0.247	0.465	0.450	0.203	0.331	0.309	0.128	0.266	0.201	0.187
S26	0.796	0.778	0.310	0.416	0.370	0.236	0.796	0.778	0.310	0.632	0.615	0.248	0.461	0.446	0.206	0.322	0.298	0.126	0.261	0.185	0.189
S27	0.799	0.786	0.313	0.413	0.355	0.233	0.799	0.786	0.313	0.625	0.607	0.247	0.459	0.431	0.203	0.320	0.297	0.123	0.260	0.187	0.188
S28	0.795	0.779	0.312	0.407	0.356	0.230	0.795	0.779	0.312	0.618	0.593	0.248	0.448	0.401	0.200	0.318	0.293	0.116	0.254	0.192	0.183
S29	0.793	0.778	0.312	0.403	0.343	0.229	0.793	0.778	0.312	0.614	0.594	0.244	0.446	0.416	0.197	0.310	0.295	0.117	0.252	0.185	0.185
S30	0.788	0.768	0.313	0.400	0.339	0.228	0.788	0.768	0.313	0.607	0.583	0.244	0.443	0.398	0.197	0.310	0.276	0.121	0.249	0.182	0.181
FF	2.659	2.461	0.881	1.999	1.970	0.394	2.659	2.461	0.881	2.138	2.147	0.394	2.151	2.145	0.475	1.792	1.760	0.267	1.954	1.975	0.306
SHE	2.843	2.852	0.703	2.798	2.799	0.527	2.843	2.852	0.703	3.050	3.040	0.547	2.912	3.017	0.536	2.785	2.757	0.470	2.408	2.410	0.332
TC	3135.545	3038.000	1074.108	2762.810	2652.000	824.157	3135.545	3038.000	1074.108	3247.000	3143.000	966.812	2888.774	2892.000	612.061	2663.833	2592.000	599.695	2228.231	1960.000	839.183

MANOVA ANOVA Post-hoc tests

Effect	Multivariate tests, effect sizes and powers (5_class)						
	Test	Value	F	Effect df	Error df	p	Partial Eta-squared
Intercept	Wilks	0	782167.3	41.000	142	0	0.999996
	Pillai	1	782166.9	41.000	142	0	0.999996
	Hotelling	225837	782167.3	41.000	142	0	0.999996
	Roy	225837	782167.3	41.000	142	0	0.999996
Group	Wilks	0	4.4	164.000	568.8288	0	0.557681
	Pillai	1.8	2.9	164.000	580	0	0.451066
	Hotelling	8.7	7.5	164.000	562	0	0.68551
	Roy	7.3	25.8	41.000	145	0	0.87937

Effect	Univariate tests (5_class)												
	Df	F470 SS	F470 MS	F470 F	F470 p	F780 SS	F780 MS	F780 F	F780 p	DFA SS	DFA MS	DFA F	DFA p
Intercept	1	518.6817	518.6817	1703.076	0	1045.009	1045.009	2343.247	0	38.43598	38.43598	7398.752	0
Group	4	99.4324	24.8581	81.621	0	64.707	16.177	36.273	0	0.35181	0.08795	16.93	0
Error	182	55.4292	0.3046			81.166	0.446			0.94548	0.00519		
All	186	154.8616				145.873				1.29728			

Effect	Df	VMS SS	VMS MS	VMS F	VMS p	R4 SS	R4 MS	R4 F	R4 p	P1 SS	P1 MS	P1 F	P1 p
Intercept	1	14.14206	14.14206	45.34722	0	4125.471	4125.471	993.6423	0	95095.5	95095.52	192.0927	0
Group	4	15.70211	3.92553	12.58739	0	1551.9	387.975	93.4459	0	82664.3	20666.06	41.7454	0
Error	182	56.75883	0.31186			755.64	4.152			90099.1	495.05		
All	186	72.46093				2307.54				172763.4			

Effect	Df	P2 SS	P2 MS	P2 F	P2 p	RR SS	RR MS	RR F	RR p	DET SS	DET MS	DET F	DET p
Intercept	1	4688.6	4688.595	137.571	0	0.143526	0.143526	196.5413	0	158.2748	158.2748	760501.5	0
Group	4	4783.9	1195.976	35.0919	0	0.102764	0.025691	35.1807	0	0.0091	0.0023	10.9	0
Error	182	6202.79	34.081			0.132907	0.00073			0.0379	0.0002		
All	186	10986.7				0.235671				0.0469			

Effect	Df	ENTR SS	ENTR MS	ENTR F	ENTR p	LMAX SS	LMAX MS	LMAX F	LMAX p	LAM SS	LAM MS	LAM F	LAM p
Intercept	1	1108.415	1108.415	20275.55	0	1.28E+09	1.28E+09	712.8365	0	153.69	153.69	145525.2	0
Group	4	1.996	0.499	9.13	0.000001	1.03E+08	2.58E+07	14.3543	0	0.0548	0.0137	13	0
Error	182	9.95	0.055			3.27E+08	1.80E+06			0.1922	0.0011		
All	186	11.946				4.30E+08				0.247			

Effect	Df	TT SS	TT MS	TT F	TT p	MSE SS	MSE MS	MSE F	MSE p	S7 SS	S7 MS	S7 F	S7 p
Intercept	1	8779.451	8779.451	2141.055	0	31025.27	31025.27	798.9813	0	31.08245	31.08245	829.8244	0
Group	4	144.041	36.01	8.782	0.000002	5164.11	1291.03	33.2473	0	4.13013	1.03253	27.566	0
Error	182	746.296	4.101			7067.25	38.83			6.81711	0.03746		
All	186	890.337				12231.36				10.94724			

Effect	Df	S8 SS	S8 MS	S8 F	S8 p	S9 SS	S9 MS	S9 F	S9 p	S10 SS	S10 MS	S10 F	S10 p
Intercept	1	33.82671	33.82671	830.7206	0	36.07684	36.07684	837.6825	0	37.93111	37.93111	840.5676	0
Group	4	4.61395	1.15349	28.3275	0	5.00643	1.25161	29.0616	0	5.35365	1.33841	29.6597	0
Error	182	7.41099	0.04072			7.83827	0.04307			8.21286	0.04513		
All	186	12.02494				12.84471				13.56651			

Effect	Df	S11 SS	S11 MS	S11 F	S11 p	S12 SS	S12 MS	S12 F	S12 p	S13 SS	S13 MS	S13 F	S13 p
Intercept	1	39.43004	39.43004	836.9327	0	40.6712	40.6712	828.2949	0	41.72909	41.72909	826.9931	0
Group	4	5.74025	1.43506	30.4603	0	6.08344	1.52086	30.9733	0	6.34263	1.58566	31.4248	0
Error	182	8.57449	0.04711			8.93662	0.0491			9.1835	0.05046		
All	186	14.31474				15.02007				15.52613			

Effect	Df	S14 SS	S14 MS	S14 F	S14 p	S15 SS	S15 MS	S15 F	S15 p	S16 SS	S16 MS	S16 F	S16 p
Intercept	1	42.58454	42.58454	821.5475	0	43.18434	43.18434	810.207	0	43.43267	43.43267	807.6284	0
Group	4	6.68885	1.67221	32.2606	0	6.91004	1.72751	32.4108	0	7.14216	1.78554	33.202	0
Error	182	9.43389	0.05183			9.70067	0.0533			9.7876	0.05378		
All	186	16.12274				16.61071				16.92976			

Effect	Df	S17 SS	S17 MS	S17 F	S17 p	S18 SS	S18 MS	S18 F	S18 p	S19 SS	S19 MS	S19 F	S19 p
Intercept	1	43.79899	43.79899	791.0651	0	44.01879	44.01879	789.5424	0	43.88314	43.88314	774.1144	0
Group	4	7.41546	1.85387	33.4831	0	7.60672	1.90168	34.1095	0	7.80634	1.95158	34.4267	0
Error	182	10.07681	0.05537			10.14692	0.05575			10.31725	0.05669		
All	186	17.49228				17.75364				18.12359			

Effect	Df	S20 SS	S20 MS	S20 F	S20 p	S21 SS	S21 MS	S21 F	S21 p	S22 SS	S22 MS	S22 F	S22 p
Intercept	1	43.65499	43.65499	768.6834	0	43.55325	43.55325	756.4018	0	43.12399	43.12399	740.4046	0
Group	4	7.92621	1.98155	34.8915	0	8.05494	2.01373	34.9731	0	8.21022	2.05255	35.2407	0
Error	182	10.33613	0.05679			10.47947	0.05758			10.60037	0.05824		
All	186	18.26234				18.53441				18.81059			

Effect	Df	S23 SS	S23 MS	S23 F	S23 p	S24 SS	S24 MS	S24 F	S24 p	S25 SS	S25 MS	S25 F	S25 p
Intercept	1	42.82046	42.82046	737.004	0	41.88972	41.88972	725.8079	0	41.84728	41.84728	714.4879	0
Group	4	8.26105	2.06526	35.5463	0	8.47667	2.11917	36.7181	0	8.37984	2.09496	35.7687	0
Error	182	10.57433	0.0581			10.50406	0.05771			10.65967	0.05857		
All	186	18.83538				18.98073				19.03951			

Effect	Df	S26 SS	S26 MS	S26 F	S26 p	S27 SS	S27 MS	S27 F	S27 p	S28 SS	S28 MS	S28 F	S28 p
Intercept	1	40.91786	40.91786	701.1788	0	40.61812	40.61812	694.6365	0	39.6158	39.6158	686.3488	0
Group	4	8.47369	2.11842	36.3018	0	8.60742	2.15185	36.8003	0	8.60366	2.15092	37.2649	0
Error	182	10.62076	0.05836			10.64225	0.05847			10.50497	0.05772		
All	186	19.09445				19.24967				19.10864			

Effect	Df	S29 SS	S29 MS	S29 F	S29 p	S30 SS	S30 MS	S30 F	S30 p	FF SS	FF MS	FF F	FF p
Intercept	1	39.05633	39.05633	682.6337	0	38.47401	38.47401	670.1706	0	765.7183	765.7183	2103.306	0
Group	4	8.72169	2.18042	38.1098	0	8.58977	2.14744	37.4058	0	21.4787	5.3697	14.75	0
Error	182	10.41298	0.05721			10.44849	0.05741			66.2579	0.3641		
All	186	19.13467				19.03825				87.7366			

Effect	Df	SHE SS	SHE MS	SHE F	SHE p	TC SS	TC MS	TC F	TC p
Intercept	1	1311.812	1311.812	4023.522	0	1.34E+09	1.34E+09	1725.498	0
Group	4	6.234	1.559	4.781	0.001087	2.08E+07	5.19E+06	6.672	0.000049
Error	182	59.339	0.326			1.42E+08	7.78E+05		
All	186	65.573				1.62E+08			

Tukey HSD Post-hoc tests

Cell no.	Tukey HSD Post-hoc tests (unequal N); Variable F470 (5_class) Error: MS between groups = .30456, df = 182.00					
	Group	{1}	{2}	{3}	{4}	{5}
1	Controls		0.086175	0.000017	0.000017	0.000017
2	CMPI	0.086175		0.000091	0.000017	0.000017
3	CMPII	0.000017	0.000091		0.000026	0.000216
4	CMPIII	0.000017	0.000017	0.000026		0.999473
5	OA	0.000017	0.000017	0.000216	0.999473	

Cell no.	Tukey HSD Post-hoc tests (unequal N); Variable DFA (5_class) Error: MS between groups = .00519, df = 182.00					
	Group	{1}	{2}	{3}	{4}	{5}
1	Controls		0.256605	0.004677	0.000017	0.000203
2	CMPI	0.256605		0.702038	0.001031	0.137144
3	CMPII	0.004677	0.702038		0.050407	0.812650
4	CMPIII	0.000017	0.001031	0.050407		0.623070
5	OA	0.000203	0.137144	0.812650	0.623070	

Cell no.	Tukey HSD Post-hoc tests (unequal N); Variable F780 (5_class) Error: MS between groups = .44597, df = 182.00					
	Group	{1}	{2}	{3}	{4}	{5}
1	Controls		0.644768	0.000030	0.000017	0.000017
2	CMPI	0.644768		0.011640	0.000017	0.000017
3	CMPII	0.000030	0.011640		0.035794	0.006960
4	CMPIII	0.000017	0.000017	0.035794		0.943417
5	OA	0.000017	0.000017	0.006960	0.943417	

Cell no.	Tukey HSD Post-hoc tests (unequal N); Variable VMS (5_class) Error: MS between groups = .31186, df = 182.00					
	Group	{1}	{2}	{3}	{4}	{5}
1	Controls		1.000000	0.668924	0.064422	0.000017
2	CMPI	1.000000		0.730109	0.148166	0.000018
3	CMPII	0.668924	0.730109		0.802265	0.000164
4	CMPIII	0.064422	0.148166	0.802265		0.008416
5	OA	0.000017	0.000018	0.000164	0.008416	

Cell no.	Tukey HSD Post-hoc tests (unequal N); Variable R4 (5_class) Error: MS between groups = 4.1519, df = 182.00					
	Group	{1}	{2}	{3}	{4}	{5}
1	Controls		0.977649	0.000083	0.000017	0.000017
2	CMPI	0.977649		0.002123	0.000017	0.000017
3	CMPII	0.000083	0.002123		0.000017	0.000017
4	CMPIII	0.000017	0.000017	0.000017		0.079671
5	OA	0.000017	0.000017	0.000017	0.079671	

Cell no.	Tukey HSD Post-hoc tests (unequal N); Variable P1 (5_class) Error: MS between groups = 495.05, df = 182.00					
	Group	{1}	{2}	{3}	{4}	{5}
1	Controls		0.999675	0.101052	0.000017	0.000017
2	CMPI	0.999675		0.204035	0.000017	0.000017
3	CMPII	0.101052	0.204035		0.001304	0.000017
4	CMPIII	0.000017	0.000017	0.001304		0.002146
5	OA	0.000017	0.000017	0.000017	0.002146	

Cell no.	Tukey HSD Post-hoc tests (unequal N); Variable P2 (5_class) Error: MS between groups = 34.081, df = 182.00					
	Group	{1}	{2}	{3}	{4}	{5}
1	Controls		0.999880	0.465158	0.000017	0.000017
2	CMPI	0.999880		0.617123	0.000017	0.000017
3	CMPII	0.465158	0.617123		0.000017	0.000020
4	CMPIII	0.000017	0.000017	0.000017		0.978906
5	OA	0.000017	0.000017	0.000020	0.978906	

Cell no.	Tukey HSD Post-hoc tests (unequal N); Variable RR (5_class) Error: MS between groups = .00073, df = 182.00					
	Group	{1}	{2}	{3}	{4}	{5}
1	Controls		0.000128	0.000017	0.000017	0.000017
2	CMPI	0.000128		0.167116	0.006434	0.158309
3	CMPII	0.000017	0.167116		0.745676	0.999971
4	CMPIII	0.000017	0.006434	0.745676		0.854759
5	OA	0.000017	0.158309	0.999971	0.854759	

Cell no.	Tukey HSD Post-hoc tests (unequal N); Variable DET (5_class) Error: MS between groups = .00021, df = 182.00					
	Group	{1}	{2}	{3}	{4}	{5}
1	Controls		0.667651	0.024182	0.000025	0.000736
2	CMPI	0.667651		0.566762	0.022218	0.058922
3	CMPII	0.024182	0.566762		0.502442	0.734927
4	CMPIII	0.000025	0.022218	0.502442		0.999383
5	OA	0.000736	0.058922	0.734927	0.999383	

Cell no.	Tukey HSD Post-hoc tests (unequal N); Variable ENTR (5_class) Error: MS between groups = .05467, df = 182.00					
	Group	{1}	{2}	{3}	{4}	{5}
1	Controls		0.513378	0.019710	0.000115	0.001954
2	CMPI	0.513378		0.679416	0.140331	0.183132
3	CMPII	0.019710	0.679416		0.833352	0.889416
4	CMPIII	0.000115	0.140331	0.833352		0.999999
5	OA	0.001954	0.183132	0.889416	0.999999	

Cell no.	Tukey HSD Post-hoc tests (unequal N); Variable LMAX (5_class) Error: MS between groups = 1796E3, df = 182.00					
	Group	{1}	{2}	{3}	{4}	{5}
1	Controls		0.126264	0.000729	0.000017	0.000053
2	CMPI	0.126264		0.626677	0.083897	0.130765
3	CMPII	0.000729	0.626677		0.758200	0.857835
4	CMPIII	0.000017	0.083897	0.758200		0.999983
5	OA	0.000053	0.130765	0.857835	0.999983	

Cell no.	Tukey HSD Post-hoc tests (unequal N); Variable MSE (5_class) Error: MS between groups = 38.831, df = 182.00					
	Group	{1}	{2}	{3}	{4}	{5}
1	Controls		0.269492	0.000021	0.000017	0.000017
2	CMPI	0.269492		0.041383	0.000025	0.000017
3	CMPII	0.000021	0.041383		0.168668	0.018253
4	CMPIII	0.000017	0.000025	0.168668		0.842647
5	OA	0.000017	0.000017	0.018253	0.842647	

Cell no.	Tukey HSD Post-hoc tests (unequal N); Variable LAM (5_class) Error: MS between groups = .00106, df = 182.00					
	Group	{1}	{2}	{3}	{4}	{5}
1	Controls		0.729850	0.021754	0.000018	0.000196
2	CMPI	0.729850		0.479860	0.003859	0.017292
3	CMPII	0.021754	0.479860		0.266073	0.550093
4	CMPIII	0.000018	0.003859	0.266073		0.997939
5	OA	0.000196	0.017292	0.550093	0.997939	

Cell no.	Tukey HSD Post-hoc tests (unequal N); Variable S7 (5_class) Error: MS between groups = .03746, df = 182.00					
	Group	{1}	{2}	{3}	{4}	{5}
1	Controls		0.649906	0.000138	0.000017	0.000017
2	CMPI	0.649906		0.043003	0.000030	0.000017
3	CMPII	0.000138	0.043003		0.198082	0.023739
4	CMPIII	0.000017	0.000030	0.198082		0.849245
5	OA	0.000017	0.000017	0.023739	0.849245	

Cell no.	Tukey HSD Post-hoc tests (unequal N); Variable TT (5_class) Error: MS between groups = 4.1005, df = 182.00					
	Group	{1}	{2}	{3}	{4}	{5}
1	Controls		0.396678	0.015866	0.000163	0.002848
2	CMPI	0.396678		0.752255	0.241236	0.309951
3	CMPII	0.015866	0.752255		0.897687	0.942312
4	CMPIII	0.000163	0.241236	0.897687		0.999996
5	OA	0.002848	0.309951	0.942312	0.999996	

Cell no.	Tukey HSD Post-hoc tests (unequal N); Variable S8 (5_class) Error: MS between groups = .04072, df = 182.00					
	Group	{1}	{2}	{3}	{4}	{5}
1	Controls		0.632478	0.000101	0.000017	0.000017
2	CMPI	0.632478		0.037643	0.000027	0.000017
3	CMPII	0.000101	0.037643		0.193315	0.022155
4	CMPIII	0.000017	0.000027	0.193315		0.843821
5	OA	0.000017	0.000017	0.022155	0.843821	

Cell no.	Tukey HSD Post-hoc tests (unequal N); Variable S14 (5_class) Error: MS between groups = .05183, df = 182.00					
	Group	{1}	{2}	{3}	{4}	{5}
1	Controls		0.403102	0.000027	0.000017	0.000017
2	CMPI	0.403102		0.032308	0.000022	0.000017
3	CMPII	0.000027	0.032308		0.160230	0.017486
4	CMPIII	0.000017	0.000022	0.160230		0.846553
5	OA	0.000017	0.000017	0.017486	0.846553	

Cell no.	Tukey HSD Post-hoc tests (unequal N); Variable FF (5_class) Error: MS between groups = .36405 df = 182.00					
	Group	{1}	{2}	{3}	{4}	{5}
1	Controls		0.010740	0.008082	0.000017	0.000253
2	CMPI	0.010740		0.999991	0.201753	0.806584
3	CMPII	0.008082	0.999991		0.132411	0.764348
4	CMPIII	0.000017	0.201753	0.132411		0.870732
5	OA	0.000253	0.806584	0.764348	0.870732	

Cell no.	Tukey HSD Post-hoc tests (unequal N); Variable S29 (5_class) Error: MS between groups = .05721 df = 182.00					
	Group	{1}	{2}	{3}	{4}	{5}
1	Controls		0.040047	0.000017	0.000017	0.000017
2	CMPI	0.040047		0.066739	0.000036	0.000018
3	CMPII	0.000017	0.066739		0.164816	0.027648
4	CMPIII	0.000017	0.000036	0.164816		0.903492
5	OA	0.000017	0.000018	0.027648	0.903492	

Cell no.	Tukey HSD Post-hoc tests (unequal N); Variable SHE (5_class) Error: MS between groups = .32604 df = 182.00					
	Group	{1}	{2}	{3}	{4}	{5}
1	Controls		0.656137	0.989391	0.992996	0.047206
2	CMPI	0.656137		0.896338	0.413270	0.000492
3	CMPII	0.989391	0.896338		0.906109	0.012563
4	CMPIII	0.992996	0.413270	0.906109		0.119440
5	OA	0.047206	0.000492	0.012563	0.119440	

Cell no.	Tukey HSD Post-hoc tests (unequal N); Variable S30 (5_class) Error: MS between groups = .05741 df = 182.00					
	Group	{1}	{2}	{3}	{4}	{5}
1	Controls		0.037654	0.000017	0.000017	0.000017
2	CMPI	0.037654		0.077512	0.000050	0.000018
3	CMPII	0.000017	0.077512		0.186034	0.028619
4	CMPIII	0.000017	0.000050	0.186034		0.887937
5	OA	0.000017	0.000018	0.028619	0.887937	

Cell no.	Tukey HSD Post-hoc tests (unequal N); Variable TC (5_class) Error: MS between groups = 7784E2 df = 182.00					
	Group	{1}	{2}	{3}	{4}	{5}
1	Controls		0.989803	0.805995	0.155193	0.001959
2	CMPI	0.989803		0.549857	0.096726	0.000315
3	CMPII	0.805995	0.549857		0.853753	0.054020
4	CMPIII	0.155193	0.096726	0.853753		0.385136
5	OA	0.001959	0.000315	0.054020	0.385136	